Electrostatic Potential as a Harbinger of Cation Coordination: $CF_3SO_3^-$ Ion as a Model Example

Shridhar P. Gejji,*,† C. H. Suresh,† Libero J. Bartolotti,‡ and Shridhar R. Gadre†

Department of Chemistry, University of Pune, Pune 411 007, India, and North Carolina Supercomputing Center, 3021, Cornwallis Road, Research Triangle Park, North Carolina 27709

Received: November 8, 1996; In Final Form: April 6, 1997[⊗]

The topography of molecular electrostatic potential (MESP) has been proposed as a predictive tool for studying ion-pair formation, using the trifluromethanesulfonate (triflate) ion, $CF_3SO_3^-$ (Tf^-), as a test example. A model based on electrostatic docking of the cation (Li^+, Na^+, NH_4^+) has been developed for studying the different possible coordinating geometries for these ion pairs. The interaction energies of different ion-pair structures estimated by the electrostatic docking model have been found to reproduce about 85% of the corresponding ab initio interaction energies. Furthermore, the geometries predicted by the present model indeed provide a good initial guess for a subsequent ab initio Hartree−Fock calculation. Ab initio local minima are usually found close to the respective geometries derived from the electrostatic docking, the bidentate structure being the most favored one. The topography-based approach thus seems to offer insights into primitive patterns of ion-pair formation. Electron correlation and the expansion of the basis set do not bring about any significant change in the MESP topography of the anion. The interionic bonds in the $NH_4^+Tf^-$, however, are relatively sensitive to the electron correlation.

1. Introduction

Alkali-metal triflates dissolved in poly(propylene oxide) (PPO) or poly(ethylene oxide) (PEO) exhibit high ionic conductivity, suggesting their use in a great number of possible technological applications.[1] The role of ion pairs in the underlying ion-transport phenomenon is a topic of considerable recent interest.[2] The structure and the energetics of the different cation−anion or polymer−cation ion pairs is one of the important factors in understanding various molecular interactions in these polymer electrolyte systems. Formation of neutral ion pairs or higher aggregates decreases the number of charge carriers, whereas the presence of charged, associated species results in the change in ionic mobility of the associated charge carriers, thereby affecting the ionic conductivity. In polyether complexes, e.g., PPO or PEO complexed with the metal salts,[3] the metal ion may interact with the polymer fragment or alternatively with the polyatomic anions. Vibrational spectroscopy provides a useful means for studying these molecular interactions in polymer salt complexes.[4] Considering the predominantly electrostatic nature of these interactions, it is felt that the use of scalar fields, for example, molecular electron densities (MED) or molecular electrostatic potentials (MESP)[5] derived from the ab initio quantum-chemical calculations may be of help in understanding them. The MESP has been shown to bring out regions of electron localization that may be attributed to a delicate balance between the nuclear and electronic contributions.[5,6] Thus the MESP exhibits rich topographical features. Gadre and co-workers[7] have recently characterized the sizes and shapes of anions from such topographical considerations. The net atomic charges derived from these MESP have been used in molecular modeling.[8] The use of MESP in understanding molecular interactions in a variety of systems, for example, experimentally explored[9] van der Waals complexes or hydrogen-bonded systems has been gaining importance in the recent years. Solid polymer electrolytes composed of PEO or PPO complexed with a salt of low lattice energy provide yet another example of the systems wherein the electrostatic interactions are very important. The triflate anion ($CF_3SO_3^-$, abbreviated hereinafter as Tf^-) which was commonly used in these electrolytes is of undoubted interest because of its unusual properties. It is seen to be thermally and chemically stable.[10,11] It shows a low tendency to form ion pairs and a strong resistance to both reductive and oxidative cleavage.[11] It was therefore felt worthwhile to probe the electron localization features of the anion in terms of the MESP topography in order to understand its cation coordination.

Some of the important questions addressed in the present work are: How important are the electrostatic interactions in deciding the structure of ion pairs? What is the role of CF_3 group of the triflate anion in the cation coordination? Is it possible to obtain reasonable estimates of the interaction energies for the different cation coordinating geometries of the Tf^- ion pairs from the electrostatic considerations alone?

In the present work, we have analyzed different possible geometries of the M^+Tf^- (M = Li, Na and NH_4) ion pairs predicted exclusively by the MESP distribution of the anion. This was achieved by an electrostatic docking of the cation around the critical point sites of the MESP. The validity of this approach was tested by subsequent single-point ab initio MO calculations at the HF/6-31G(d) level. The model presented here is relatively simple, requires less computer time, and engenders different possible geometries for the ion pairs. Some of these turned out to be transition states, saddles, and maxima on the potential energy surface as may be seen from the calculations of the vibrational frequencies. The computational method and the results are presented in the following sections.

2. Computational Method

The MESP, $V(\mathbf{r})$, at a point $\mathbf{r}$ due to a molecular system with nuclear charges $\{Z_A\}$ located at $\{\mathbf{R_A}\}$ and electron density $\rho(\mathbf{r})$ is given by

† University of Pune.
‡ North Carolina Supercomputing Center.
[⊗] Abstract published in *Advance ACS Abstracts,* July 1, 1997.

S1089-5639(96)03744-9 CCC: $14.00

$$V(\mathbf{r}) = \sum_{A}^{N} \frac{Z_A}{|\mathbf{r} - \mathbf{R}_A|} - \int \frac{\rho(\mathbf{r}')\, d^3r'}{|\mathbf{r} - \mathbf{r}'|} \quad (1)$$

where N is the total number of nuclei in the molecule. The first and the second terms in the above equation refer to the bare nuclear potential and electronic contributions, respectively. Topological features of a function of many variables are characterized by the gradient field. Topological analysis[7] of $V(\mathbf{r})$ is based on the identification and location of the critical points (CPs), the points at which $\nabla V(\mathbf{r}) = 0$. The rank of the CP is given by the number of nonzero eigenvalues of the Hessian matrix **A**, the elements of which are defined by

$$A_{ij} = \left.\frac{\partial^2 V(\mathbf{r})}{\partial x_i\, \partial x_j}\right|_{\mathbf{r}=\mathbf{r}_c} \quad (2)$$

where $\mathbf{r}_c$ is a critical point. The Poisson equation, $\nabla^2 V(\mathbf{r}) = 4\pi\rho(\mathbf{r})$ (excluding the nuclear sites) provides a check on the trace of the Hessian matrix. If none of the eigenvalues of the Hessian matrix is zero, then the CP is said to be nondegenerate. A nondegenerate[7] CP is characterized by an ordered pair (R, σ) where R is the rank of matrix **A** and σ the signature, which is the algebraic sum of the signs of the eigenvalues. A nondegenerate CP of rank 3 corresponds to one of the following four possible types: (3,−3), (3,−1), (3,+1), (3,+3). The CP corresponding to $\sigma = -3$ refers to a maximum. A CP of (3,−1) or (3,+1) type corresponds to a saddle point, while a CP of signature +3 arises due to a local minimum.

In the present work, the 6-31G (d) ab initio Hartree−Fock (HF) wave function, obtained with the GAUSSIAN 94 package[12] is used for the evaluation of the MESP of the anion. The MESP is calculated by using the FORTRAN program INDPROP,[13] and the three-dimensional visualization of the MESP topography of the Tf^- was carried out on a PC-486 computer with the FORTRAN program UNIVIS.[14] Docking of the cation, e.g., Li^+, Na^+, and NH_4^+, at different sites around the MESP critical points of the free Tf^-, was carried out in order to predict the structure of the M^+Tf^- (M = Li, Na and NH_4) complex in different coordinating geometries.

Assuming the interaction of a cation and the Tf^- to be predominently electrostatic, the corresponding interaction energy is given by

$$E_{\text{dock}}^{\text{int}} = \int V_A(\mathbf{r})\, \rho_c(\mathbf{r})\, d^3r \quad (3)$$

where V_A refers to the electrostatic potential of the anion and ρ_c defines the charge density of the cation at that site. Thus the cation coordination can be viewed as a molecular recognition problem where the ion pairs are treated as electrostatic LOCK (anion) and KEY (cation) complexes. The present electrostatic interaction model bears some similarity with the one developed earlier by Kahn et al.[15] for interaction of neutral molecules. However, the docking procedure is implemented here for a cation−anion pair and is discussed below.

The initial sites for cation coordinations are provided by the positions of the MESP critical points. In fact, this is a unique feature of the method emerging from the richness of the anionic MESP topography. The optimum energy structures for the M^+Tf^- ion pairs were derived by minimizing the $E_{\text{dock}}^{\text{int}}$ through the translation and rotation (only for NH_4^+) of the cation. During these operations, the internal geometries of the anion and cation were kept intact. The distance of the approaching cation from Tf^- was limited by the CP nearest to the outer atoms, viz., oxygens and fluorines of the anion. For the inner atoms, the respective van der Waals radii[16] (3.31 and 3.2 au, respectively, for the sulfur and carbon) were used, and the standard ionic radii[16] were used for the cations. The geometries, thus obtained by minimizing $E_{\text{dock}}^{\text{int}}$, referred to hereafter as "docked geometries" were subsequently employed as starting geometries for further optimization in the ab initio framework. Here, ab initio SCF-MO calculations have been performed with the GAUSSIAN-94 program,[12] using the internally stored 6-31G(d) basis for the lithium and sodium triflate complexes. For $NH_4^+Tf^-$ a set of 2p polarization functions were added to the hydrogens in this basis. The equilibrium geometries of the M^+Tf^- complexes were obtained by the analytical gradient relaxation method. The harmonic vibrational frequencies of these complexes were computed by diagonalizing the respective force constant matrices.

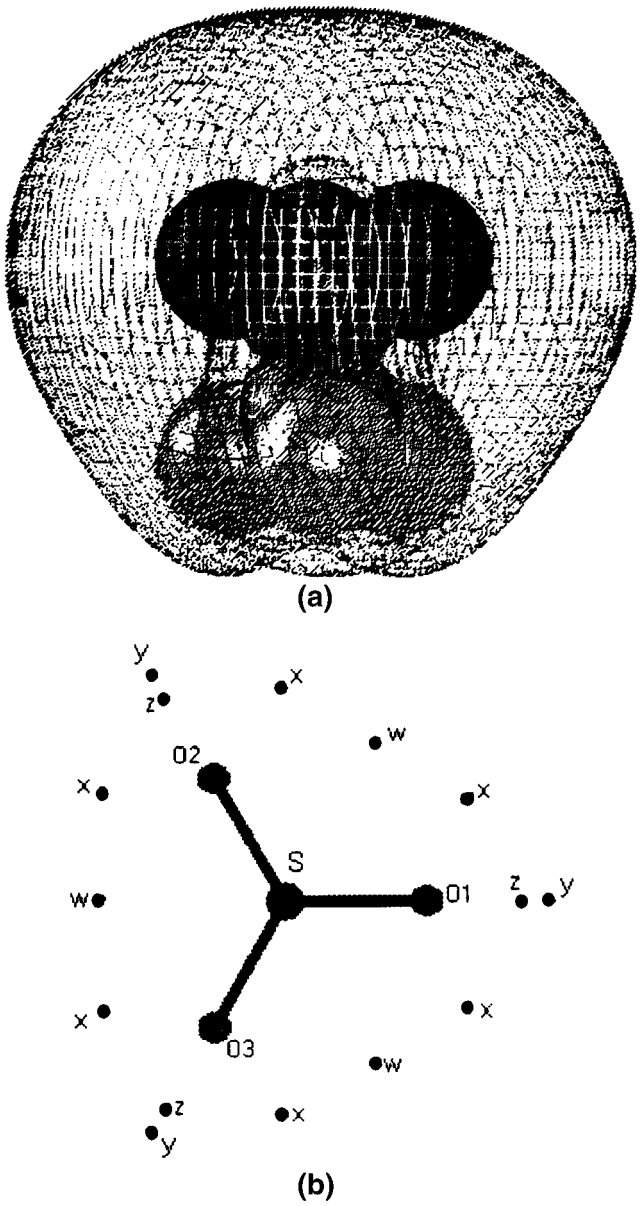

Figure 1. (a) MESP iso-surface of the triflate ion, viz. $V = -297.0$ kJ mol^{-1} encompassing the whole anion. (b) Top view of the SO_3 end of the anion showing the MESP CPs. See text for details.

MESP-driven net atomic charges for these geometries were obtained by fitting the respective MESPs on a grid of points surrounding the anion. A grid was constructed by using standard Cox and Williams[17]-type sampling algorithm. The grid containing Tf^- extends over 4 Å on either side of the anion. The FORTRAN program GRID[18] was employed for obtaining

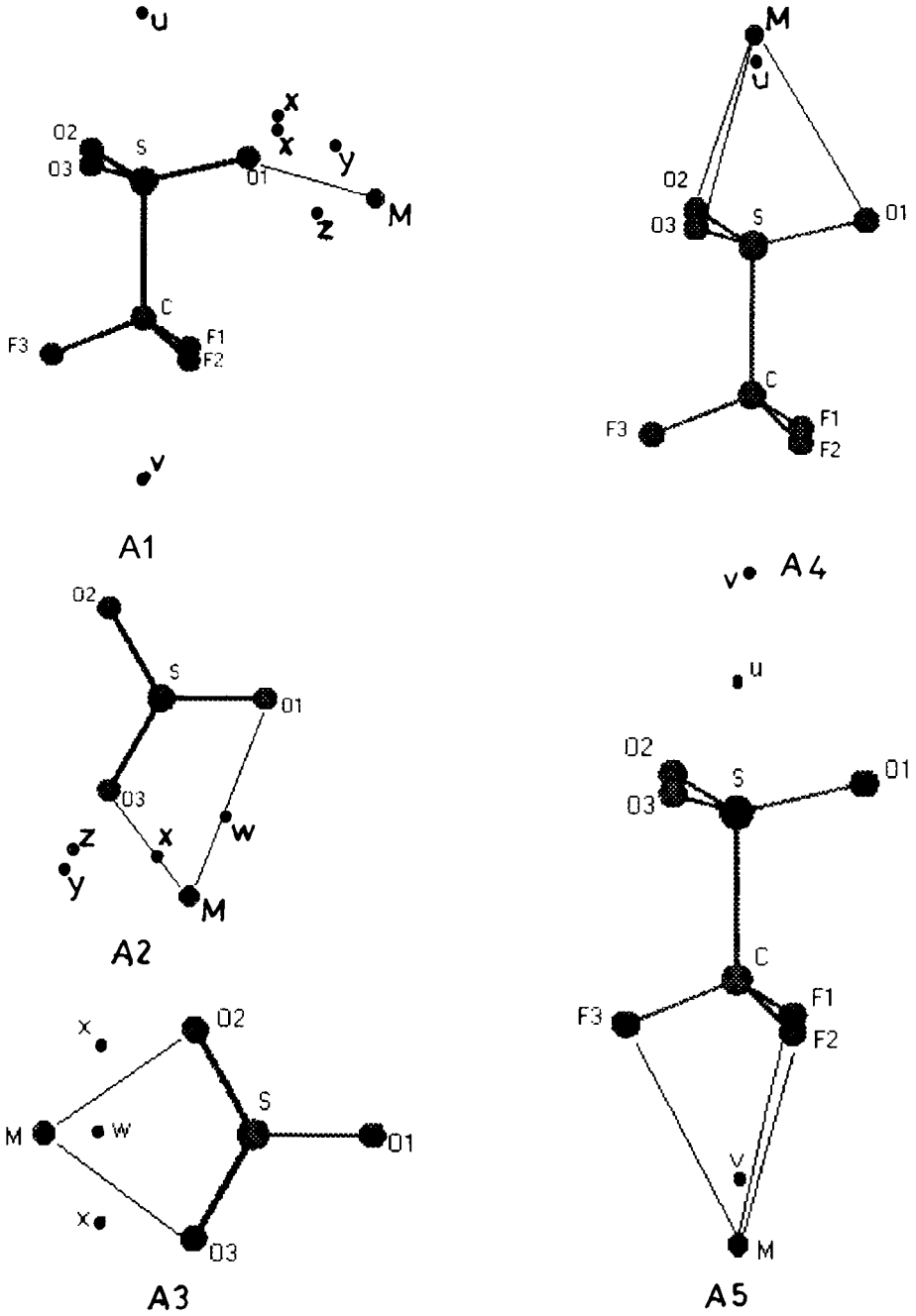

Figure 2. "Docked"geometries for the M^+Tf^- (M = Li or Na) ion pair. Only those CPs relevant to the docking of the cations are shown. See text for details.

atomic charges for different centers in the free anion as well as in different geometries of the complexes.

3. Results and Discussion

As noted above, the MESP of an anion is endowed with rich topographical features due to the presence of a large number of negative-valued CPs. In fact, all the anions should have a negative-valued MESP iso-surface encompassing the whole nuclear framework. This is in accordance with the conclusions drawn for molecular anions by Gadre and Pathak[19] through generalization of the earlier work of Politzer[20] for the atomic anions. This demands that there has to be at least one negative-valued minimum in the MESP of the molecular anions, along *any arbitrary outward (from the nuclear framework) direction*. In the present case, the most negative valued MESP iso-surface encompassing the whole anion was found around −297.0 kJ/mol (Figure 1a). The *minimal surface* defined by Gadre et al.[19] lies completely inside this surface.

The main features of the MESP topography of the triflate anion are summarized below. A top view of the SO_3 end of the anion showing the MESP CP's is depicted in Figure 1b. It shows, for each oxygen, one pair of (3,+3) MESP minima with a value of −641.8 kJ/mol typically at a distance of 2.26 au from it (denoted by *x*). The two oxygen minima are connected via a (3,+1) saddle (denoted by *y*) with $V = -607.5$ kJ/mol observed nearly along the S−O bond direction. Further, two such pairs are connected via another (3,+1) saddle (denoted by *w*) identified along a line bisecting the O−S−O bond angle ($V = -557.6$ kJ/mol). Also observed are a (3,−1) CP (with $V = -427.8$ kJ/mol) on the C_3 axis, 4.28 au away from sulfur (denoted by *u*) and another (3,−1) saddle of value −587.3 kJ/mol (denoted by *z*) just below the CP represented as *y*. In contrast to the rich topography seen at the SO_3 end (i.e., six minima and ten saddles), the CF_3 end shows no minima in the MESP topography. A (3,−1) CP on the C_3 symmetry axis (denoted by *v*) 4.18 au away from *C* ($V = -296.9$ kJ/mol) and

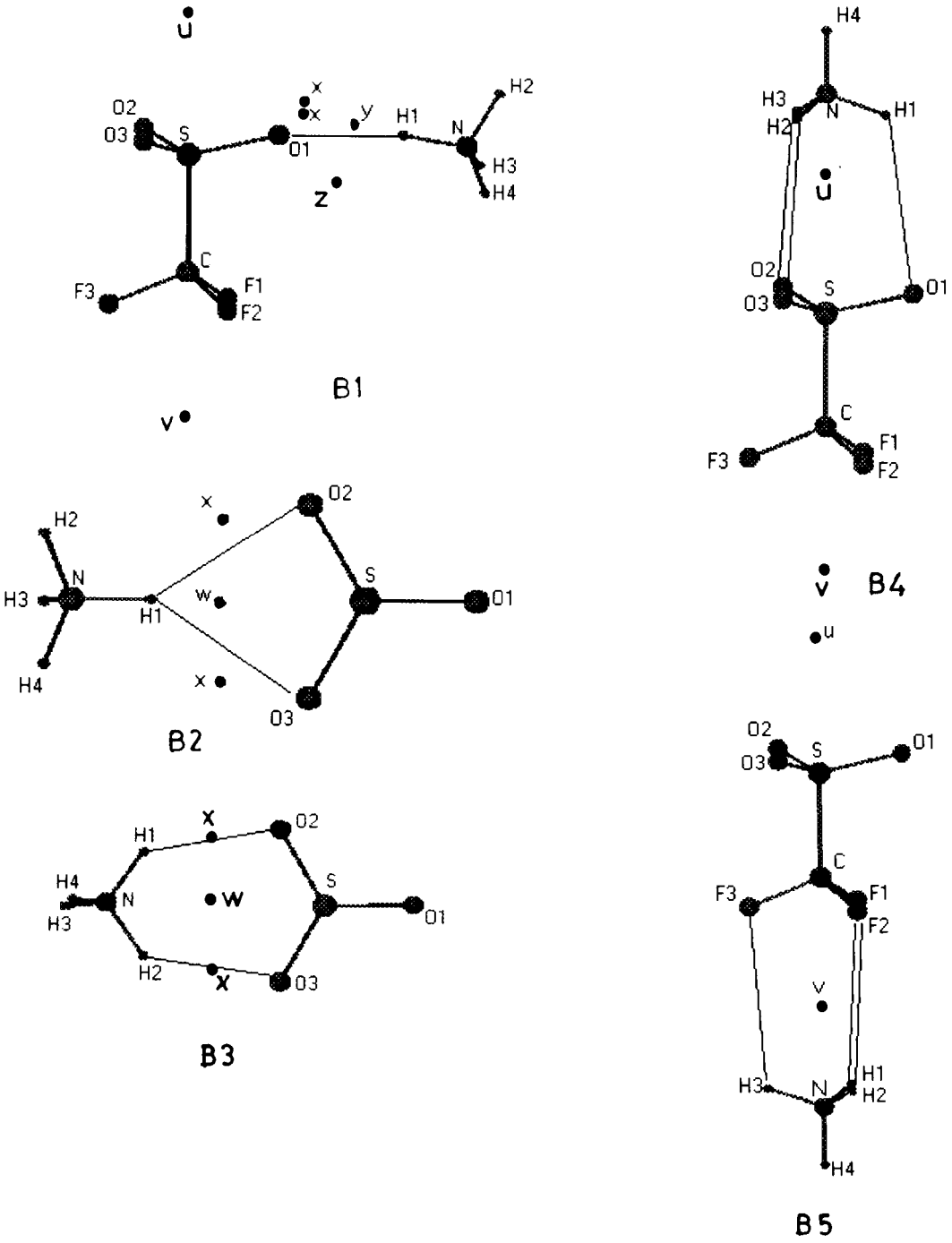

Figure 3. "Docked"geometries for the $NH_4^+Tf^-$ ion pair. Only those CPs relevant to the docking of the cations are shown. See text for details.

(3,+1) saddles along each C−F bond directions ($V = -367.2$ kJ/mol and is 2.35 au from the nearest fluorine) are observed (denoted by *t*). For notations, cf. Figure 2 and Table 7.

It may be interesting to note that although the fluorine atom is inherently more electronegative than the oxygen, the MESP at the SO_3 end of the anion is more negative as well as topographically richer than the CF_3 end, as can be noticed from the values at the critical points. The negative-valued CPs in the MESP act as attractors for the cations. Thus the MESP topographical studies presented here predict two possible bidentate (symmetric and unsymmetric) coordinated structures for the cation−triflate ion pair. When the cation approaches the (3,+3) CP, it leads to an unsymmetric bidentate structure, whereas approach toward the CP observed between two (3,+3) CPs yields a symmetric bidentate structure for the ion pair. The latter is expected to be more favorable since it enjoys more electrostatic attraction forces from the electron rich locations of the two (3,+3) CPs. The approach of the cation along the S−O bond direction toward the (3,+1) CP generates a monodentate structure (cf. Figure 2A1). Further, relatively weak tridentate structures at both the SO_3 and the CF_3 ends of the anion are also possible (cf. A4 and A5 in Figure 2) via the (3,−1) CPs. The former is expected to be relatively more stable, the MESP minimum being deeper for this case. Yet another possibility is a cation approaching toward the (3,+1) CP of the flourine (i.e., along the C−F bond direction).

The tetrahedral geometry of the ammonium cation presents a rather intricate situation. One can imagine two hydrogens of the cation being attracted toward (3,+3) CPs of the anion as a favorable situation for cation coordination. Alternatively, the approach of the ammonium ion toward the CPs located on the C_3 axis would give rise to the possibilities of tridentate coordination at the SO_3 and CF_3 ends of the anion. Further, a monodentate coordination may also be visualized by placing

TABLE 1: Initial Energies, RMS Forces and the Predicted Change in Single-Point SCF Energies and Gradients for the M^+Tf^- (M = Li, Na, and NH_4) Ion Pairs (See Text for Details)

system	coordination	initial energy (au)	RMS force (au/Å)	predicted change in energy (au)
Li^+Tf^-	monodentate at SO_3	−965.716 81	0.0233	0.0057
	bidentate at SO_3	−965.733 15	0.0279	0.0096
	tridentate at SO_3	−965.701 62	0.0219	0.0093
	tridentate at CF_3	−965.655 28	0.0160	0.0104
Na^+Tf^-	monodentate at SO_3	−1120.111 80	0.0186	0.0041
	bidentate at SO_3	−1120.128 45	0.0213	0.0054
	tridentate at SO_3	−1120.110 44	0.0174	0.0074
	tridentate at CF_3	−1120.061 23	0.0130	0.0069
$NH_4^+Tf^-$	monodentate at SO_3	−1014.975 03	0.0107	0.0019
	bidentate at SO_3	−1014.981 82	0.0128	0.0008
	tridentate at SO_3	−1014.972 84	0.0146	0.0008
	tridentate at CF_3	−1014.926 77	0.0080	0.0036

one of the hydrogens of the cation at the CPs along the S−O bond direction or the C−F bond direction as discussed earlier.

The heuristic arguments presented above clearly present different possibilities of the cation coordination in the M^+Tf^- ion pairs. The electrostatic interaction energy, E_{dock}^{int}, is obtained by using the docking model outlined in section 2. The different geometries derived from the minimization of E_{dock}^{int} for the M^+Tf^- (M = Li and Na) ion pairs are shown in Figure 2. To test the validity of this approach, these geometries of the M^+Tf^- complexes were further subjected to optimization followed by evaluation of vibrational frequencies in the ab initio HF/6-31G(d) calculations. The following inferences may be drawn. The geometries shown as A1, A3, and A4 (cf. Figure 2) lead to a transition state (monodentate), minimum (bidentate), and a saddle (tridentate at the SO_3 end) point structures, respectively, in both Li^+Tf^- and Na^+Tf^- ion pairs in the ab initio framework. On the other hand, the A5 geometry representing a tridentate coordination at the CF_3 end gives a transition state for Li^+ and a local minimum for Na^+. It, however, should be pointed out that the final optimized geometry obtained by employing the unsymmetric bidentate structure (A2) is the same as that derived from the symmetric structure (A3). The docked structure obtained at the (3,+1) CP of the fluorine (this is not shown in the figure) does not give a corresponding stationary point geometry in the ab initio MO calculations.

The initial geometries used in the optimization calculations for the NH_4^+ Tf^- are shown in Figure 3. The structures B1 (monodentate), B3 (bidentate), and B4 and B5 (tridentate at the SO_3 and CF_3 ends of the anion, respectively) led to minima on the potential energy surface (no imaginary vibrational frequency). These geometries were not very different from the starting ones with respect to the nature of cation coordination. The geometry shown in B2, representing one of the hydrogens of the NH_4^+ ion coordinating with two oxygens of the SO_3 end of the anion, was also tried. Such a coordination, however, fails to produce a stationary point geometry on the potential energy surface and finally leads to a bidentate (B3) structure. In other words, B2 and B3 both lead to the identical bidentate coordinated geometry for the $NH_4^+Tf^-$ ion-pair after optimization with the ab initio MO calculations. Interestingly, the final optimized structure obtained from the B1 geometry, showing a monodentate coordination at the SO_3 end as a guess does not represent an ion pair but shows a proton transfer from the NH_4^+ to the anion, leading thereby to the formation of triflic acid and ammonia as $NH_3 \cdot HOO_2SCF_3$. As observed in the lithium and the sodium cation coordination, a coordination at the (3,+1) CP of the fluorine failed to produce an ab initio stationary structure. The final geometry parameters of the optimized structure in this case agree well with those of the triflic acid reported earlier in the literature.[21]

Thus it may noted that the qualitative trends in ion-pair formation can be systematically investigated by the present method employing rigid individual structures of cation and anion. It may, however, be pointed out that the present model may not be successful in the cases where the anion shows a very large geometry change compared to that in the free gaseous state when interacting with the cation or when charge or proton transfer is involved. In the former case, different conformers of the anion could be probed for studying the ion-pair formation which may, at least partly, account for the effects due to geometry relaxation.

The RMS forces (energy gradients with respect to the nuclear coordinates) and the GAUSSIAN-predicted energy changes (i.e., the difference in the SCF energies in two successive iterations) obtained for these "docked" geometries of the M^+Tf^- ion pairs in different coordinating geometries are presented in Table 1. In most of the cases, the predicted energy change and the RMS force are around 0.005 au and 0.02 au/Å, respectively. This suggests that the ab initio stationary points are generally in the vicinity of those predicted by the model.

The interaction energies from the HF/6-31G(d) were calculated in the following way: $E_{HF}^{int} = E_{ion-pair} - (E_{anion} + E_{cation})$ where $E_{ion-pair}$, E_{anion}, and E_{cation} denote the total electronic energies of the ion pair, free triflate anion, and cation, respectively. These are compared with the corresponding "docked", E_{dock}^{int} values in Table 2. It may be readily noted that the electrostatic interactions alone weigh about 85% of the actual interaction (the ab initio) energy and the energy rank order[11] of Li^+Tf^- ion-pair conformers, which follows the trend bidentate > monodentate > tridentate which agrees well with the one predicted by the ab initio calculations. Thus the

TABLE 2: Comparison of Interaction Energies from the Present Model and the HF/6-31G(d) (Complete Optimization) Calculations (See Text for Details)

system	coordination	E_{RHF} (au)	no. of imaginary frequencies	E_{dock}^{int} (kJ/mol)	E_{HF}^{int} (kJ/mol)
Li^+Tf^-	monodentate at SO_3	−965.725 74	1	−501.0	−558.7
	bidentate at SO_3	−965.746 96	0	−537.7	−613.8
	tridentate at SO_3	−965.716 61	2	−427.6	−535.1
	tridentate at CF_3	−965.665 67	1	−289.7	−397.9
Na^+Tf^-	monodentate at SO_3	−1120.120 12	1	−438.0	−480.0
	bidentate at SO_3	−1120.136 79	0	−487.9	−524.6
	tridentate at SO_3	−1120.121 42	2	−414.4	−485.3
	tridentate at CF_3	−1120.073 22	0	−259.7	−356.7
$NH_4^+Tf^-$	monodentate at SO_3	−1014.999 44	0	−388.2	−461.7[a]
	bidentate at SO_3	−1014.997 27	0	−401.3	−456.4
	tridentate at SO_3	−1014.989 91	0	−383.0	−438.0
	tridentate at CF_3	−1014.939 23	0	−236.1	−304.3

[a] This is attributed to proton transfer and not to the ion-pair formation.

TABLE 3: HF/6-31G(d) Geometry Parameters for the M^+Tf^- (M = Li or Na) Conformers[a]

		Li^+Tf^-				Na^+Tf^-			
	Tf^-	mono at SO_3	bi at SO_3	tri at SO_3	tri at CF_3	mono at SO_3	bi at SO_3	tri at SO_3	tri at CF_3
C−S	1.817	1.823	1.813	1.812	1.851	1.824	1.812	1.810	1.842
O1−S	1.443	1.482*	1.471*	1.452*	1.430	1.471*	1.422	1.451*	1.432
O2−S	1.443	1.423	1.471*	1.452*	1.430	1.427	1.464*	1.451*	1.432
O3−S	1.443	1.423	1.418	1.452*	1.430	1.427	1.464*	1.451*	1.432
F1−C	1.323	1.294	1.308	1.307	1.351*	1.297	1.322	1.309	1.343*
F2−C	1.323	1.340	1.318	1.307	1.350*	1.341	1.309	1.309	1.343*
F3−C	1.323	1.340	1.308	1.307	1.350*	1.341	1.309	1.309	1.343*
M−O*		1.778	1.899	2.250		2.120	2.235	2.534	
		(1.794)	(1.794)	(2.350)		(2.146)	(2.313)	(2.702)	
M−F*					2.023				2.356
					(2.447)				(3.070)
O1−S−C	102.60	97.17	103.75	108.27	99.80	98.50	106.23	107.02	100.30
O2−S−C	102.60	104.60	103.75	108.27	99.80	103.82	103.10	107.20	100.29
O3−S−C	102.60	104.60	106.64	108.27	99.81	103.82	103.10	107.20	100.29
F1−C−S	111.80	115.63	110.30	109.60	115.84	114.99	109.34	109.92	114.72
F2−C−S	111.80	109.14	109.39	109.60	115.92	109.94	110.85	109.92	114.72
F3−C−S	111.80	109.14	110.31	109.60	115.94	109.94	110.85	109.92	114.72
M−O1−S		120.46	89.28	180.0		122.55	93.73	73.82	
		(149.61)	(112.63)	(180.0)		(152.95)	(88.85)	(77.40)	
M−F1−C					79.75				83.52
					(81.68)				(88.19)
O2−S−C−O1	120.0	116.80	109.96	120.0	120.00	117.56	123.66	120.0	240.0
O3−S−C−O1	240.0	243.20	234.98	240.0	240.00	242.00	236.34	120.0	120.0
F1−C−S−O1	180.0	180.0	185.42	180.0	180.01	180.0	180.0	240.0	180.0
F2−C−S−O1	300.0	303.52	304.97	300.0	299.93	302.96	299.40	300.0	300.0
F3−C−S−O1	60.0	56.48	64.53	60.0	60.07	57.04	60.60	60.0	60.0
M−O1−S−C		0.0	107.56	0.0		0.0	106.52	180.0	
		(0.0)	(92.83)	(0.0)		(0.0)	(93.46)	(180.0)	
M−F1−C−S					180.00				180.0
					(180.00)				(180.)

[a] The numbers in parentheses indicate those predicted from the present model. See text for details

predominant role of electrostatic interactions in the ion-pair formation is clearly brought out. The "predicted" energy rank order of the Na^+Tf^- conformers is, however, slightly different.

The optimized geometries for the stationary points of the M^+Tf^- (M = Li and Na) ion pairs are reported in Table 3 along with the geometrical parameters obtained from the docking model (listed in parentheses). As pointed out in section 2, the HF/6-31G(d) geometry of the free Tf^- was kept intact, when the electrostatic docking was implemented in all these coordinating geometries of these ion pairs. The MESP-predicted "docked" geometries show a fairly good overall agreement with those derived from the full optimization in the HF/6-31G(d) calculations. The largest deviation up to ~0.17 Å may be noted for the M−O1 bond distances. The M−O1 distances follow the order mono- < bi- < tri- dentate coordination in the ab initio calculations. The predicted M−O1 distances from the present model for the Li^+Tf^- in mono- and bidentate coordinations, however, are nearly the same. This probably is an artifact of imposing the constraint of the distance of closest approach of the cation to the anion described in the preceding section. Consideration of bond angle parameters reveals the difference for the M−O−S bond angles to be as large as 30° in the different coordinating geometries of these ion pairs. The dihedral angles are nearly unchanged in most of the cases.

The geometrical parameters of the $NH_4^+Tf^-$ complex from the ab initio theory and the electrostatic docking are compared in Table 4. The monodentate coordination represents quite a different situation due to proton transfer in the ab initio calculation representing $NH_3 \cdot HOO_2SCF_3$ and *not the ion pair*. The bi- and tridentate coordinated geometrical parameters of H1···O1 show a larger variation of nearly 0.45 Å. The bond angles generally show a good agreement.

The undoubted importance of the MESP in cation coordination as discussed above suggests that the net atomic charges

TABLE 4: HF/6-31G(d,p) Geometry Parameters for the $NH_4^+Tf^-$ Complexes (Numbers in Parentheses Indicate Those Predicted from the Present Model)

	Tf^-	$NH_4^+Tf^-$			
		mono	bi	tri at SO_3	tri at CF_3
C−S	1.817	1.814	1.810	1.809	1.831
O1−S	1.443	1.537*	1.462*	1.451*	1.434
O2−S	1.443	1.414	1.424	1.451*	1.434
O3−S	1.443	1.414	1.462*	1.451*	1.434
F1−C	1.323	1.313	1.311	1.311	1.338*
F2−C	1.323	1.306	1.311	1.311	1.338*
F3−C	1.323	1.307	1.320	1.311	1.338*
H1−O1		0.999	1.768	2.147	
		(1.686)	(2.226)	(2.640)	
H1− F1					2.119
					(3.077)
O1−S−C	102.60	106.78	103.18	105.96	100.75
O2−S−C	102.60	100.15	105.80	105.96	100.75
O3−S−C	102.60	106.17	103.18	105.96	100.75
F1−C−S	111.80	109.45	110.74	110.16	113.64
F2−C−S	111.80	110.51	110.74	110.16	113.64
F3−C−S	111.80	109.37	109.82	110.16	113.64
H1−O1−S		113.09	114.48	93.67	
		(162.57)	(110.16)	(92.69)	
H1− F1−C					105.91
					(106.68)
O2−S−C−O1	120.0	114.64	122.56	120.0	120.0
O3−S−C−O1	240.0	228.84	245.11	239.93	240.0
F1−C−S−O1	180.0	187.06	177.03	180.0	180.01
F2−C−S−O1	300.0	307.06	297.88	300.0	300.01
F3−C−S−O1	60.0	67.58	57.46	60.0	60.01
H1−O1−S−C		98.79	248.35	179.99	
		(179.63)	(267.53)	(179.93)	
H1− F1−C−S					180.00
					(180.00)

shown in Table 5 derived from the MESP could be useful in molecular modeling. For the free anion the net atomic charges on C, S, O, and F turn out to be 0.065, 1.109, −0.629, and −0.097, respectively. A comparison of Li^+Tf^- and Na^+Tf^-

TABLE 5: MESP-Driven Net Atomic Charges in au for Free Tf^- and for the Lowest Energy Minima of the M^+Tf^- (M = Li, Na, and NH_4)

	CF_3SO_3	$LiCF_3SO_3$	$NaCF_3SO_3$	$NH_4CF_3SO_3$
C	0.065	0.283	0.310	0.129
S	1.109	1.020	0.975	1.152
O1	−0.629	−0.681	−0.667	−0.690
O2	−0.629	−0.681	−0.667	−0.690
O3	−0.629	−0.483	−0.494	−0.548
F1	−0.097	−0.089	−0.105	−0.069
F2	−0.097	−0.089	−0.105	−0.069
F3	−0.097	−0.142	−0.153	−0.106

TABLE 6: Streching Vibrational Frequencies in cm^{-1} of the Tf^- in Different M^+Tf^- Ion Pairs from the HF Calculations[a]

(a) Tridentate Coordination at the SO_3 and CF_3 Ends of the Anion

			the cation at the SO_3 end			the cation at the CF_3 end		
		free anion	Li^{+b}	Na^{+b}	NH_4^+	Li^{+c}	Na^+	NH_4^+
SO_3	ss	1127	1136	1131	1124	1151	1145	1141
SO_3	as	1343	1335	1340	1338	1447	1438	1429
CF_3	ss	1424	1402	1409	1416	1407	1407	1412
CF_3	as	1398	1424	1415	1410	1201	1234	1262

(b) Monodentate Coordination at SO_3 End

		Li^+Tf^{-d}	Na^+Tf^{-d}
SO	s	1099	1114
SO_2	s	1329	1342
SO_2	s	1485	1469
CF_2	s	1261	1258
CF_2	s	1356	1353
CF	s	1485	1470

(c) Bidentate Coordination at SO_3 End

		Li^+Tf^-	Na^+Tf^-	$NH_4^+Tf^-$
SO_2	s	1103	1108	1107
SO_2	s	1251	1278	1270
CF	s	1386	1368	1376
CF_2	s	1405	1411	1411
CF_2	s	1424	1416	1412
SO	s	1471	1456	1476

[a] ss - symmetric stretching, as - asymmetric stretching, s - stretching). See text for details. [b] Shows two imaginary frequencies. [c] Shows one imaginary frequecy. [d] Shows one imaginary frequency.

shows that the difference in the net atomic charges of sulfur and the coordinated oxygen is 0.339 and 0.308, respectively. This indicates more weakening of the S−O1 bond in Li^+Tf^- than Na^+Tf^- and therefore more stronger interaction for the former. This is consistent with the interaction energies presented in Table 2. The situation with the $NH_4^+Tf^-$ is, however, quite different since there are two oxygens connecting the cation via the two hydrogen bonds.

One may wonder at this juncture, how significant are the basis-set and correlation effects in deciding the structure and energetics of the ion pairs? The effect of expansion of basis set by adding diffuse functions and that of the electron correlation via the Moller−Plesset second-order perturbation (MP2) method on the MESP topography has also been explored. The HF and MP2 MESP values at CPs and the distances of CPs from the nearest atom are compared with those obtained from the HF/6-31G(d) calculations in Tables 7 and 8, respectively. It may readily be noticed that the CPs are nearly insensitive to the increase in the basis set size beyond the 6-31G-(d), as has been noticed earlier[23,24] by Kulkarni and Gadre. The typical deviations in the MESP values and CP distances at these sites being ∼5%. The bond angles and the dihedral angles a CP make with the nearest atoms show a maximum deviation within 3° from the average value. Since the MESP topography

TABLE 7: MESP CPs of the Tf^-[a]

		MESP value			
CP	type	*A*	*B*	*C*	*D*
x	(3,+3)	−0.2447	−0.2366	−0.2385	−0.2362
y	(3,+1)	−0.2316	−0.2250	−0.2259	−0.2231
z	(3,−1)	−0.2239	−0.2184	−0.2151	−0.2090
w	(3,+1)	−0.2126	−0.2045	−0.2170	−0.2143
u	(3,−1)	−0.1629	−0.1572	−0.1714	−0.1678
t	(3,+1)	−0.1402	−0.1383	−0.1391	−0.1399
v	(3,−1)	−0.1132	−0.1122	−0.1189	−0.1200

[a] A, B, and C represent the CP values at HF/6-31G(d), HF/6-31G+(d), and MP2/6-31G(d)//HF/6-31G(d) levels. D represents those obtained at MP2/6-31G(d)//MP2/6-31G(d) level.

TABLE 8: MESP CP Distances of Tf^- from the Nearest Atom in Å (Notations as in Table 7)

	A	*B*	*C*	*D*
p1−O1	1.196	1.220	1.228	1.232
p2−O1	1.196	1.225	1.222	1.227
p3−O1	1.220	1.250	1.246	1.261
p4−O2	1.743	1.778	1.720	1.740
p5−S	2.268	2.340	2.159	2.182
p6−F1	1.245	1.287	1.269	1.267
p7−F1	2.116	2.184	2.023	2.025

TABLE 9: Some MP2-Optimized Bond Distances for the M^+Tf^- (Li, Na, and NH_4)[a]

bond distances	Tf^-	Li^+Tf^- (bi)	Na^+Tf^- (bi)	Na^+Tf^- (tri at CF_3 end)	$NH_4^+Tf^-$ (bi)	$NH_4^+Tf^-$ (tri at CF_3 end)
C−S	1.835	1.831	1.839	1.883	1.830	1.860
O1−S	1.477	1.508*	1.498*	1.467*	1.493*	1.470
O2−S	1.477	1.508*	1.498*	1.467*	1.457	1.470
O3−S	1.477	1.451	1.455	1.467*	1.513*	1.470
F1−C	1.353	1.335	1.334	1.389	1.339	1.380*
F2−C	1.353	1.351	1.385	1.389	1.339	1.367*
F3−C	1.353	1.335	1.334	1.389	1.350	1.380*
M−O*		1.912	2.298			
M−F*				2.623		

[a] The starred values indicate atoms involved in interionic bonds. All values in Å. See text for details.

is almost unchanged in the more sophisticated calculations, it may be expected that the predicted trends in structure and energetics of different ion-pair conformers at HF/6-31G (d) level will be preserved.

Further assessement of the above arguments may be done partially by studying the effects of correlation on the minimum energy conformers of the M^+Tf^- (M = Li, Na, NH_4) ion pairs. This has been done by optimizing these geometries at MP2 level with the 6-31G(d) basis within the frozen core approximation using GAUSSIAN 94. Some geometry parameters are enlisted in Table 9. Inclusion of the MP2 correlation does not change the geometrical parameters significantly for the Tf^- and the M^+Tf^- (M = Li, Na) ion pairs. The C−F and S−O bonds are elongated by ∼0.03 Å in all these ion pairs when the correlation is added. The agreement for the different bond angle and dihedral angle parameters at the HF and MP2 levels for M = Li or Na is within 1°.

Unlike the case of monatomic cation- Tf^- ion-pairs the $NH_4^+Tf^-$ at the MP2 level show a significant change in geometry from the HF level of theory. The bi- and tridentate (at the CF_3 end) coordinating geometries reveal unequal interionic bond lengths. The H···O interionic bonds in bidentate structure are 1.506 and 1.826 Å, whereas the H···F distances in the tridentate structure are 1.907, 1.907, and 2.346 Å. The bond or the dihedral angle change is within 5°. The $NH_4^+Tf^-$ conformer showing the tridentate coordination at the SO_3 end

TABLE 10: M^+Tf^- Ion-Pair Energies in au[a]

energy	M = Li	M = Na	M = Na	M = NH_4	M = NH_4
$E°_{HF}$	−965.512 97	−1119.936 72	−1119.936 72	−1014.822 96	−1014.822 96
$E°_{MP2}$	−966.866 75	−1121.291 59	−1121.291 59	−1016.368 13	−1016.368 13
E^1_{HF}	−965.746 96	−1120.136 79 (bi)	−1120.073 22 (tri at CF_3)	−1014.997 27 (bi)	−1014.939 23 (tri at CF_3)
E^1_{MP2}	−967.111 31	−1121.501 42 (bi)	−1121.436 85 (tri at CF_3)	−1016.555 65 (bi)	−1016.497 21 (tri at CF_3)
E_{HF}^{int}	−0.2340	−0.2001	−0.1365	−0.1743	−0.1163
E_{MP2}^{int}	−0.2446	−0.2098	−0.1453	−0.1875	−0.1291

[a] $E°_{HF}$ and $E°_{MP2}$ denote sum of energies of the ions and E^1_{HF} and E^1_{MP2} represent the energies of the ion-pairs whereas the E_{HF}^{int} and E_{MP2}^{int} are the interaction energies at HF and MP2 levels. See text for details. $E_{HF}^{int} = E^1_{HF} - E°_{HF}$, $E_{MP2}^{int} = E^1_{MP2} - E°_{MP2}$

as obtained in the HF calculation converges finally to the bidentate structure at the MP2 level.

Total electronic and interaction energies derived from the single-point full MP2 calculations, obtained at the frozen core MP2 geometries, are presented in Table 10. For Li^+Tf^-, as a test example, the frozen core MP2 energy was −967.074 63 au as compared to its HF counterpart −965.746 96 au. The full MP2 calculations including the core orbitals leads to the total energy of −967.111 36 au. Inclusion of the core orbitals thus brings about a very significant change in the binding energies of the ion pair. On the other hand, single-point full MP2 calculations with the frozen core MP2 geometries show a deviation of 0.000 05 au in the binding energies from the full MP2 optimizations. Thus due care has been taken in comparing the binding energies at MP2 level reported in Table 10. These interaction energies for the ion pairs are typically 0.01 au lower than the HF values.

The HF/6-31G(d) vibrational frequencies of internal stretching vibrations of Tf^- in the tridentate coordination, the cation being coordinated via the SO_3 end, are presented in Table 6a. Although the SO_3 coordinating ammonium triflate exhibits a *local minimum*, no such minima were found for the lithium or sodium triflates. The M^+Tf^- (M = Li and Na) ion pairs in these geometries have two imaginary frequencies, suggesting that these represent *second-order saddle points* on the potential energy surface. The symmetric SO_3 stretching was used as a probe to distinguish the different coordinating geometries of the triflate ion.[22] The symmetric SO_3 stretching in the Li^+Tf^- and Na^+Tf^- ion pairs show frequency upshift when compared with that of the free anion, whereas for the $NH_4^+Tf^-$ ion pair a downshift (of nearly 3 cm^{-1}) is noted. The SO_3 normal vibration in these ion-pairs are strongly coupled with the C−S stretching vibrations. The vibrational frequencies for the CF_3 coordinating geometries for the M^+Tf^- ion-pairs are also reported in Table 6a. The frequencies of the normal vibrations of the monodentate M^+Tf^- (M = Li and Na) are presented in Table 6b. These represent a *transition state* (with one imaginary frequency) on the potential energy surface. Both these structures show frequency upshifts with respect to the free anion. As noted earlier, the $NH_4^+Tf^-$ monodentate combination leads to the proton transfer from NH_4^+ to the anion. For the minimum energy structures of the M^+Tf^- ion pairs, the different stretching vibrational frequencies are given in Table 6c. The free triflate anion belongs to C_{3v} symmetry point group. The asymmetric SO_3 vibration is degenerate. When the cation interacts with the Tf^-, lowering of the symmetry results in the frequency shift of the symmetric SO_3 stretching[22] and the splitting of degenerate SO_3 vibration may be observed as well. The magnitude of these frequency shifts or the splitting of degenerate normal vibration provide a measure of the strength of the interaction. The normal vibrations of the anion in these ion-pair geometries are, however, strongly coupled.[11] Thus, a correlation of the strength of the cation interaction with the predicted frequency shift of the symmetric SO_3 stretching vibration or alternatively, with the magnitude of splitting of the degenerate SO_3 stretching of the anion is far from straightforward. To discuss these frequency shifts in quantitative terms, the electron correlation from the second-order Moller−Plesset (MP2) or more sophisticated theory has to be included in the frequency calculations which is outside the scope of the present work.

4. Concluding Remarks

The present work brings out the importance of MESP in cation coordination: the anionic MESP topography as well as MESP-driven charges are used with the model. The negative valued MESP CPs of the anion act as the cation attractors. The essential MESP topographical features of Tf^- are seen to be almost invariant beyond 6-31G(d) level basis within HF and MP2 framework. The MESP value at these CP is an indicator of the strength of such interactions. The cation coordination in the triflate anion is mainly via the SO_3 end. A weak coordination from the CF_3 end is also possible for the ammonium and sodium ions. The structures and energetics of the different conformers based on simple electrostatic considerations are in good agreement with those predicted by the respective ab initio HF/6-31G(d) calculations except, perhaps in situation wherein the relaxation and correlation effects are expected to play a larger role. The preferred geometry for the M^+Tf^- ion pair is seen to occur with the cation in bidentate coordination. In fact, the "docked" geometries derived from the model presented here invariably serve as very good starting points for the corresponding ab initio calculations. The GAUSSIAN-predicted energy changes and the RMS force of almost all these geometries typically turn out to be around 0.005 au and 0.02 au/Å, respectively. The MESP thus acts as a harbinger to cation coordination predicting the different minima, transition-state and saddle-point structures of the ion pairs on the potential energy surface. The triflate ion presented here just serves as a test example: larger anions open up enormous possibilities for the cation interaction sites. The present model based on electrostatic considerations yields a finer tool for the *systematic investigations* of the structure and energetics of the different ion-pair conformers. Being currently explored are larger anionic and model polymer systems for cation coordination.

Acknowledgment. S.R.G. and C.H.S. are grateful to the Council of Scientific and Industrial Research (CSIR), New Delhi, and S.P.G. is thankful to the University Grants Commission (UGC), New Delhi, India for financial assistance.

References and Notes

(1) (a) Gray, F. M. *Solid Polymer Electrolytes, Fundamentals and Technological Applications*; VCH: New York, 1991; p 3. (b) Armand, M. B. *Annu. Rev. Mater. Sci.* **1986**, *16*, 245. (c) MacCallum , J. R.; Vincent, C. A. *Polmer Electrolyte Reviews*; MacCallum, J. R., Vincent, C. A., Eds.; Elsevier: New York, 1987; Vol. 1, Chapter 2. (d) Armand, M. B.; Chabagno, V. M.; Duclot, M. J. *Fast Ion Transport in Solids*; Vashishta, P., Mundy, N. J., Shenoy, G. K., Eds.; Elsevier: North-Holland: NewYork, 1979; p 131. (e) Shriver, D. F.; Papka, B. L.; Ratner, M. A.; Dupon, R.; Wong, T.; Brodwin, M. *Solid State Ionics* **1985**, *5*, 83. (f) Weston, J. E.; Steele, B. C. H. *Solid State Ionics* **1982**, *7*, 81. (g) Adamic, K. J.; Greenbaum, S. G.;

Wintersgill, M. C.; Fontanella, J. J. *J. Appl. Phys.* **1986**, *60*, 1342. (h) Subbarao, E. C. *Solid Electrolytes and Their Applications*; Plenum: New York, 1980.

(2) (a) Bernson, A.; Lindgren, J. *Solid State Ionics* **1993**, *60*, 37. (b) Katsuhara, Y.; Hammakar, R. M.; Desmarteau, D. D. *Inorg. Chem.* **1980**, *19*, 607. (c) Kakihana, M.; Sandahl, J.; Schantz , S.; Torell, L. M. *Proc. Second Intern. Symp. Polymer Electrolytes*; Scrosati, B., Ed.; Elsevier: Amsterdam, 1990.

(3) (a) Ratner, M. A. *Polymer Electrolyte Reviews*; MacCallum, J. R., Vincent, C. A., Eds.; Elsevier: New York, 1987; Vol. 1, p 235. (b) Dupon, R.; Papke, B. L.; Ratner, M. A.; Whitmore, D. H.; Shriver, D. F. *J. Am. Chem. Soc.* **1982**, *104*, 6247. (c) Papke, B. L.; Ratner, M. A.; Shriver, D. F. *J. Electrochem. Soc.* **1982**, *129*, 1434. (d) Schantz, S.; Torell, L. M.; Stevens, J. R. *J. Appl. Phys.* **1988**, *64*, 2038. (e) Schantz, S.; Sandhal, J.; Borjesson, L.; Torell, L. M.; Stevens, J. R. *Solid State Ionics* **1988**, *28*−*30*, 1047. (f) Frech, R.; Huang, W. *Solid State Ionics* **1993**, *66*, 183.

(4) (a) Frech, R.; Manning, J. P. *Electrochim. Acta* **1992**, *37*, 1499. (b) Manning, J.; Frech R. *Polymer* **1992**, *33*, 3487. (c) Bernson, A.; Lindgren, J.; Huang, W.; Frech, R. *Polymer* **1995**, *36*, 4471.

(5) (a) Politzer, P. *Chemical Applications of Atomic and Molecular Electrostatic Potentials*; Politzer, P., Ed.; Plenum: New York, 1981. (b) Bonaccorsi, R.; Scrocco, E.; Tomasi, J. *J. Chem. Phys.* **1970**, *52*, 5270. (c) For a study of YXH_4-type complexes employing electrostatic considerations, see: Bonaccorsi, R.; Scrocco, E.; Tomasi, J. *Theor. Chim. Acta* (Berlin) **1979**, *52*, 113. (d) Nàray-Szabo, G.; Ferenczy, G. G. *Chem. Rev.* **1995**, *4*, 829.

(6) (a) Gadre, S. R.; Kulkarni, S. A.; Shrivastava, I. H. *J. Chem. Phys.* **1992**, *31*, 5253. (b) Kulkarni, S. A.; Gadre, S. R. *J. Mol. Struct. (THEOCHEM)* **1996**, *361*, 83.

(7) (a) Gadre, S. R.; Shrivastava, I. H. *J. Chem. Phys.* **1991**, *94*, 4384. (b) Gadre, S. R.; Kölmel, C.; Ehrig, M.; Ahlrichs, R. Z. *Naturforsch.* **1993**, *48a*, 145.

(8) (a) Williams, D. E. *J. Comput. Chem.* **1994**, *15*, 719. (b) Chipot, C.; Angyan, J. G.; Ferenczy, G. G.; Scheraga, H. A. *J. Phys. Chem.* **1993**, *97*, 6628. (c) Chirlian, L. E.; Francl, M. M. *J. Comput. Chem.* **1987**, *8*, 894. (d) Gadre, S. R.; Shrivastava, I. H. *Chem. Phys. Lett.* **1993**, *204*, 350.

(9) (a) Read, W. G.; Campbell, E. J.; Henderson, G. *J. Chem. Phys.* **1983**, *78*, 3501. (b) Crabtree, R. H. *Chem. Rev.* **1995**, *95*, 987. (c) Andrews, A. M.; Hillig II, K. W.; Kuczkowski, R. L. *J. Am. Chem. Soc.* **1992**, *114*, 6765. (d) Mielke, Z.; Tokahadze, K. G.; Latajaka, Z.; Ratajczak, E. *J. Phys. Chem.* **1996**, *100*, 539. (e) Worthand , G. A.; Wade , R. C. *J. Phys. Chem.* **1995**, *99*, 17473. (f) Gadre, S. R.; Bhadane, P. K.; Pundlik, S. S.; Pingale, S. S. In *Molecular Electrostatic Potentials*: *Concepts and Applications*; Murray, J. N., Sen, K. D., Eds.; Elsevier: Amsterdam, 1996; Chapter 5. (g) See: Buckingham A. D.; Fowler P. W. *J. Chem. Phys.* **1983**, *79*, 6426. Buckingham A. D.; Fowler P. W. *Can. J. Chem.* **1985**, *63*, 2018, for a significant theoretical study of weakly bonded complexes.

(10) Haszeldine, R. N.; Kidd, J. M. *J. Chem. Soc.* **1954**, 4228.

(11) (a) Gejji, S. P.; Hermansson, K.; Lindgren, J. *J. Phys. Chem.* **1993**, *97*, 3712. (b) Huang, W.; Wheeler, R. A.; Frech, R. *Spectrochim Acta* **1994**, *50A*, 985. (c) Benrabah, D.; Arnaud, R.; Sanchez, J.-Y. *Electrochim. Acta* **1995**, *40*, 2437. (d) Arnaud, R.; Benrabah, D.; Sanchez, J.-Y. *J. Phys. Chem.* **1996**, *100*, 10882. (e) For recent related work on $LiClO_4$, see: Klassen, R.; Aroca, R.; Nazri, G. A. *J. Phys. Chem.* **1996**, *100*, 9334.

(12) *GAUSSIAN 94*; Frisch, M. J.; Trucks, G. W.; Schlegel, H. B.; Gill, P. M. W.; Johnson, P. G.; Robb, M. A.; Cheeseman, J. R.; Keith, T. A.; Petersson, G. A.; Montgomery, J. A.; Raghavachari, K.; Al-Laham, M. A.; Zakrzewski, V. G.; Oritz, J. V.; Foresman, J. B.; Cioslowski, J.; Stetanov, B. B.; Nanayakkara, A.; Challacombe, M.; Peng, C. Y.; Ayala, P. Y.; Chen, W.; Wong, M. W.; Andres, J. L.; Replogle, E. S.; Gomperts, R.; Martin, R. L.; Fox, D. J.; Binkley, J. S.; Defrees, D. J.; Baker, J.; Stewart, J. P.; Head-Gordon, M.; Gonzalez, C; Pople, J. A. GAUSSIAN, Inc.: Pittsburgh, PA, 1995.

(13) The package *INDPROP* developed by S. R. Gadre, and co-workers, University of Pune, 1994.

(14) Fortran code *UNIVIS* written by: Limaye, A. C.; Inamdar, P. V.; Dattwadkar, S. M.; Gadre, S. R. *J. Mol. Graphics* **1996**, *14*, 19.

(15) (a) For an electrostatic model for diene−dienophile and related interactions, see: Kahn Pau, C. F.; Chamberlin, A. R.; Hehre, W. J. *J. Am. Chem. Soc.* **1987**, *109*, 650. (b) Kahn, S. D.; Dobbs, K. D.; Hehre, W. J. *J. Am. Chem. Soc.* **1988**, *110*, 4609 and references therein.

(16) Bondi, A. *J. Phys. Chem.* **1964**, *68*, 441. (b) Pauling, L. *The Nature of Chemical Bond*; Cornell University Press: Ithaca, NY, 1942.

(17) Cox, S. R.; Williams, D. E. *J. Comput. Chem.* **1981**, *2*, 304.

(18) Chipot, C.; Angyan, J. G. *GRID* 3.0. A Fortran program performing charge fitting to molecular electrostatic potentials or fields, 1992.

(19) (a) Gadre, S. R.; Pathak, R. K. *J. Chem. Phys.* **1990**, *93*, 1770.

(20) For earlier studies on atomic anions, see: Sen, K. D.; Politzer, P. *J. Chem. Phys.* **1989**, *90*, 4070. (c) Sen, K. D.; Politzer, P. *J. Chem. Phys.* **1989**, *91*, 5123.

(21) Gejji, S. P.; Hermansson, K.; Lindgren, J. *J. Phys. Chem.* **1993**, *97*, 6986.

(22) (a) Gejji, S. P.; Hermansson, K.; Tegenfeldt, J.; Lindgren, J. *J. Phys. Chem.* **1993**, *97*, 11402. (b) Huang, W.; Frech , R.; Wheeler, R. A. *J. Phys. Chem.* **1994**, *98*, 100.

(23) Gadre S. R.; Kulkarni S. A.; Suresh, C. H.; Shrivastava, I. H. *Chem. Phys. Lett.* **1995**, *239*, 83.

(24) Kulkarni S. A. *Chem. Phys. Lett.* **1996**, *254*, 268.